



<p>Aya Mohamed Hassanien Abd Elfattah Teaching Assistant, Department of Civil Engineering, Faculty of Engineering, October 6 University, 6th of October City, Giza, Egypt.</p> <p>Dr. Mostafa Mokhtar Mostafa Assistant Professor, Irrigation and Hydraulics Department, Faculty of Engineering, Ain Shams University, Cairo, Egypt.</p> <p>Dr. Noran Mohamed Abdel Latif Assistant Professor, Civil Department - Acting Head of Civil Engineering Department, Canadian International College, CIC, Cairo, Egypt.</p> <p>Prof. Dr. Samir Ali Ead Professor, Irrigation and Hydraulics Department, Faculty of Engineering, Ain Shams University, Cairo, Egypt.</p>	<p>Title: The Influence of Finite Tailwater on The Characteristics of Plane Turbulent Wall Jets</p> <p>ABSTRACT</p> <p>This paper displays a laboratory study of plane turbulent wall jets on smooth boundaries with finite tailwater depth. The primary aim was to study the effect of changing Froude numbers on the behavior of plane turbulent wall jets with shallow tailwater depth. A series of four experiments, maintaining constant tailwater depth ratio of $y_t/b_o = 22$ and four values of Froude numbers (4, 6, 8, and 10), were conducted to observe and quantify the growth of the wall jet, the decay of the velocity scale, and the variations in discharge and momentum fluxes. The results from these experiments were compared with the classical wall jet. It was found that the characteristics of plane turbulent wall jets with shallow tailwater depth differ significantly from those of classical wall jets. The experimental results show that jets with shallow tailwater depth ratios experience faster maximum velocity decay and faster growth of the jet half width. In addition, there is an increased relative discharge with normalized longitudinal distance, but it decreases rapidly to a maximum value at the end of the eddy length. The momentum flux in the forward flow of the wall jet significantly diminishes with increasing distance from the nozzle. The decay is attributed to the entrainment of the return flow, which possesses negative momentum, and an increase in tailwater depth at a distance from the nozzle generates this return flow. This study enhances the understanding of the behavior of plane turbulent wall jets on smooth beds with finite tailwater depth.</p> <p>Keywords wall jets, finite tailwater, turbulence</p> <p>ARTICLE INFO :</p> <p>Article History: Received: xxxx xx, 20xx Accepted: xxxx xx, 20xx Available Online: xxxx xx, 20xx</p> <p>DOI : 10.21608/ijaecr.2025.356487.1034</p>
---	---



Introduction:

A classical wall jet is a jet that comes from a rectangular slot perpendicular to a bed submerged in a semi-infinite fluid medium and has a thickness b_0 and a uniform velocity U_0 (see Fig. 1). It is usually anticipated that momentum flux will be conserved. (Albertson et al. 1950; Rajaratnam 1976; Schlichting 1979). Upon the jet's exit from the slot, a shear layer forms on the fluid side, while a boundary layer emerges on the bed. The juncture of the two layers signifies the termination of the potential core, beyond which the flow becomes fully developed (see Fig. 2.a, and b). Experimental observations of the streamwise velocity (u) at various x stations revealed that the velocity profiles maintain a consistent shape across the different stations. The data from (Forthmann, 1936) indicated that, at any x station, the axial velocity u rises from zero at the bed to attain its maximum value u_m at $y = \delta$, subsequently declining to zero at greater values of y , as shown in the Fig. 2.c. The boundary layer is the area between $y = 0$ to $y = \delta$. The region above the boundary layer is called the half width of the jet b , which is similar to mixing region. The maximum velocity u_m was taken as the velocity measure to evaluate the similarity of velocity profiles and the length measure b was taken as the distance above the channel bed, where the axial velocity u equals $0.5 u_m$, as a length scale. experiments of (Miller and Comings 1957; Heskestad 1965; Goldschmidt and Eskinazi 1966; Kotsovinos 1975) revealed that the momentum flux diminished to a certain degree at considerable distances from the jet origins. (Kotsovinos, 1978) noted that the momentum flux may diminish to around 80% of its initial value at a longitudinal distance of $100b_0$ for plane turbulent jets. He ascribed this reduction to the negative momentum of the entrained fluid, which approached the jet at an angle of approximately $\pi/4$ radians from the jet's forward direction. Additionally, he also formulated an equation to characterize the fluctuation of momentum flux relative to the longitudinal distance from the jet- producing nozzle, based on an approximate integral analysis. (Swean et al. 1989) investigated the fluctuations of momentum and volume fluxes, together with the development of plane turbulent surface jets with constrained tailwater depth. They performed 10 tests to investigate the impact of finite tailwater depth on surface jet characteristics and to examine the variations in momentum and volume fluxes, as well as the disruption of the surface jet caused by the restricted ambient depth. The experimental findings of (Vanvari and Chu, 1974) and (Rajaratnam and Humphries, 1984) were also utilized. Their findings indicated a reduction in momentum and a deviation in the velocity and length scales due to jet confinement. studies by (Ead and Rajaratnam, 1998, 2001) indicate that the reduction of momentum flux is considerable, even with substantial tailwater exceeding 300 to 900 slot widths. In the case of a plane turbulent wall jet released into somewhat deep tailwater, if the shear force on the bed is disregarded, it is commonly assumed, similar to a plane free jet, that the momentum flux will be conserved (see to Rajaratnam 1976). Given that the plane wall jet model has been employed to examine various flows in hydraulic structures, even when the tailwater depth is relatively modest, it was deemed both intriguing and beneficial to investigate the fluctuations in momentum flux within a plane wall jet across a spectrum of tailwater levels, while also considering the influence of bed friction. (Javan and Namin, 2013) investigated simulated plane turbulence wall jets in shallow tailwater using a time-splitting approach on a non-staggered grid in curvilinear coordinates. The model used the $k-\epsilon$ turbulence closure model to solve the Navier-Stokes equations. They compared their numerical results with experimental results of (Ead and Rajaratnam, 2002). (Aziz and Khan, 2011) numerically investigated a turbulent, nonbuoyant vertical jet in shallow water using a three-dimensional



computation model. They verified their data from mean and turbulent flow quantities using measurements of laser Doppler velocimeters. The research by (Bey et al., 2008) examined the effects of channel width and tailwater depth on scour induced by plane wall jets. Four sets of testing were undertaken, each with differing tailwater depths. The velocity-time history was employed to identify flow regimes, and distinct velocity signature patterns were observed. The distinction between high and low submergence flow was shown to depend on jet exit velocity. Although channel width did not significantly affect flow classification, it did influence the scour pattern. (Bhuiyan et al., 2011) examined the characteristics of reattached plane turbulence offset jets in rough beds and shallow tailwater depths. The flow consisted of a deflecting free jet and a growing wall jet. The results demonstrate that offset height accelerates forward-flow momentum, local maximum velocity, and wall shear stress more swiftly in the offset jet than in plane turbulent wall jets. (Ead and Rajaratnam, 2002) and (Shabayek, 2011) examined the properties of plane turbulent wall jets with finite tailwater depth, comparing shallow and deep tailwater depth ratios. and the results clarified jet behavior in restricted fluid settings. Experiments were performed to measure the growth of the wall jet, increase and decay of velocity scale, momentum flux, and volume flux variation. (Eriksson et al., 1998) performed laser-Doppler measurements on a turbulent wall jet with a Reynolds number of 9600, focusing on the near-wall area. The study revealed significant differences in conventional turbulence intensity and shear stress, attributed to the effects of increased turbulence intensity. (Shinneeb et al., 2019) performed measurements utilizing Particle Image Velocimetry (PIV) on an isothermal circular jet entering a shallow water layer. The results demonstrated negligible horizontal confinement yet substantial vertical confinement. The velocity field was evaluated on both vertical and horizontal planes. The mean velocity field and large-scale turbulence structures were defined, with the axial velocity profile demonstrating near homogeneity across the shallow water depth. Prominent vortices were seen in the superficial layer, leading to a marginal rise in axial velocity. (Rowland et al., 2009) experimental results for a wall-bounded plane jet, analogous to jets produced by flow entering floodplain lakes, demonstrate pronounced large-scale meandering turbulent patterns. The intricate structure dominates jet turbulence, increasing turbulence intensities by 3-5 times and producing lateral shear stresses and momentum diffusivities one to two orders of magnitude greater than those generated by bed friction alone. (Francesco Secchi et al., 2023) investigated the self- similarity of mean velocity and Reynolds stresses profiles of a turbulent jet impinging onto smooth and rough surfaces at Reynolds number $Re = 10,000$. The wall jet is structured into an inner and outer layer, resembling a turbulent boundary layer and free-shear flow. The self- similarity of the profiles is marginally affected by roughness topographies, but significant scatter is observed in the mean velocity profiles scaled by inner layer units. (Shivankar et al., 2020) examined the impact of wall undulation on turbulent jet transport characteristics, considering both the wall and offset jets. The results indicate that the undulation of wall has a strong influence on altering the friction coefficient and reattachment length for offset jets. It further reveals that there is an intricate interplay between undulation height and offset ratio in dictating the flow characteristics. (Gupta et al., 2020) studied demonstrates that streamwise variations of velocity and length scales in turbulent wall jets show remarkable scaling with local parameters, indicating no imposed scales. The mean velocity profile data suggest two distinct layers: the wall layer and the full-free jet layer. Each layer scales on appropriate length and velocity scales, and the overlap of these universal scaling leads to a Reynolds-number-dependent power-law velocity variation in



the overlap layer. (Harish Choudhary et al., 2024) suggested that plane turbulent wall jets have two distinct structural modes: wall mode scaling on wall variables and free-jet mode scaling on jet variables. Experimental data from a wall jet facility revealed modal spectral contributions to variances of velocity fluctuations, Reynolds shear stress, shear force, turbulence production, velocity fluctuation triple products, and turbulent transport. The free-jet mode has wavelengths scaling on the jet length scale and contains two dominant submodes. The findings support the hypothesis of wall and free-jet structural modes and suggest a complex region below maximum velocity.

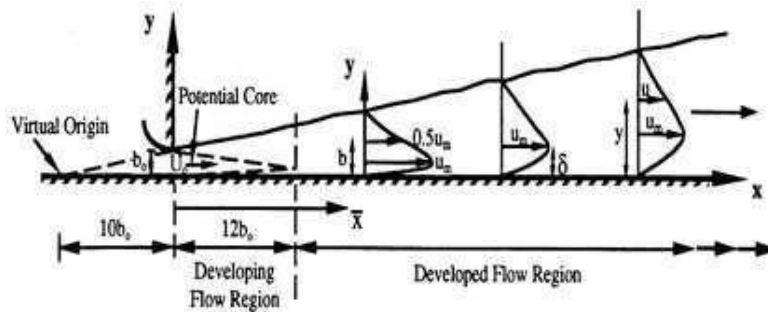
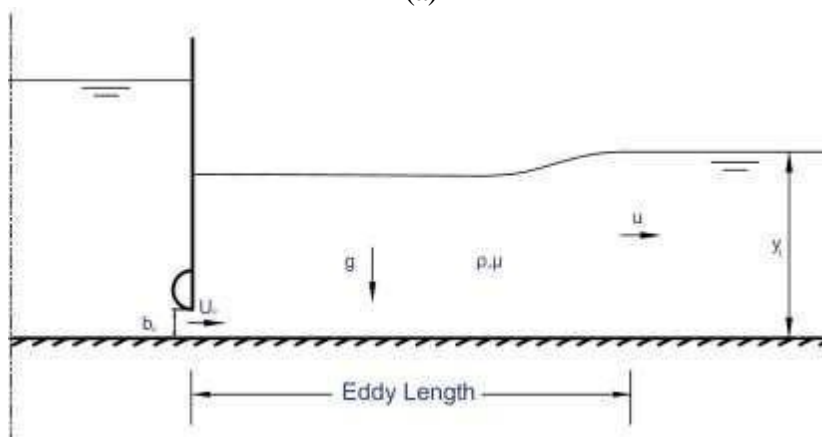
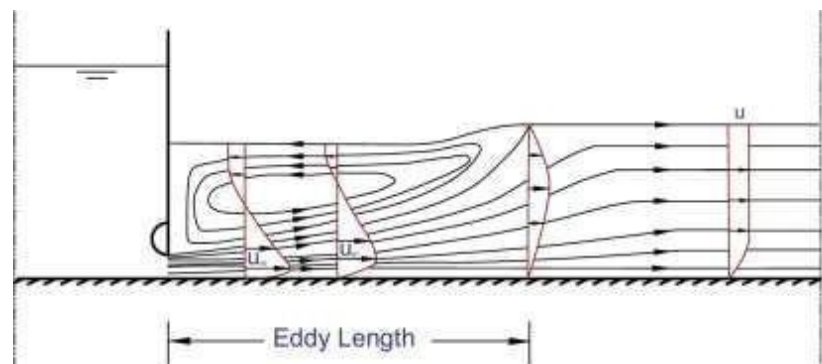


Fig. 1. Definition illustration of a classical wall jet (Ead and Rajaratnam 1999)

(a)



(b)



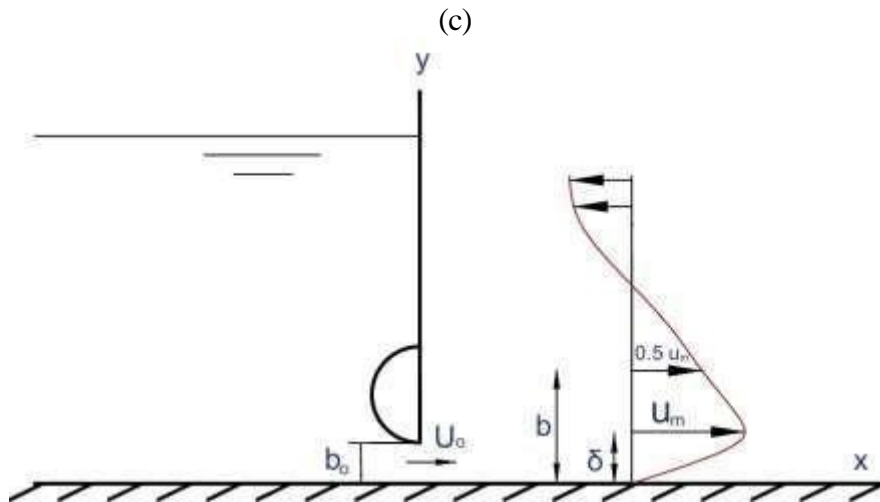


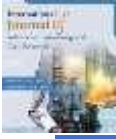
Fig. 2. (a) Definition illustration of a plane turbulent wall jet with finite tailwater depth; (b) Flow pattern; (c) Typical velocity distribution

Experimental arrangement:

Experiments were performed in a rectangular flume 0.151 m in width, 0.30 m in depth, and 2.5 m in length, featuring 13 mm thick clear Plexiglas sides and a steel bed covered with plastic sheets. All experiments were conducted on a horizontal surface. A single-leaf head gate featuring a streamlined lip was employed to generate a supercritical flow with a thickness equivalent to the gate opening, b_0 . A tailgate, positioned at the downstream end of the flume, was utilized to regulate the tailwater depth, while a centrifugal pump was used to recirculate the flow. One valve was installed to regulate the discharge. Four experiments (1 to 4) were conducted, with four different Froude numbers and the essential details of these experiments are presented in Table 1. A Prandtl tube with an external diameter of 3.0 mm was employed to measure the time-averaged longitudinal velocity u along vertical sections at various longitudinal distances from the jet- producing opening. The Prandtl tube was affixed to a manometer board mounted on the flume's side wall. All measurements were conducted in the central third of the flume, and the values of the Froude numbers in the four experiments are (4, 6, 8, and 10), The Reynolds number of the jet ranged from (12528 to 31321). For large values of the Reynolds number, viscous effects can be neglected.

Table 1. Primary Details of Experiments

Expt.	b_0 (cm)	W (cm)	y_t (cm)	U_0 (m/s)	Q_0 (L/s)	Fr	Re
1	1	15.1	22	1.25	1.9	4	12528
2				1.88	2.8	6	18793
3				2.5	3.8	8	25057
4				3.13	4.7	10	31321



Dimensional analysis:

Considering the problem illustrated in Fig. 2.a, any characteristic (\emptyset) of the wall jet can be expressed as a function of various parameters of the flow and fluid dimensions as follows:

$$\emptyset = f_1 (b_0, U_0, g, y_t, \rho, \mu) \tag{1}$$

where g = acceleration due to gravity, ρ = mass density and μ = dynamic viscosity of the fluid. Using the Pi theorem, it can be shown that

$$\emptyset = f_2 \left(\frac{U_0}{\sqrt{g b_0}}, \frac{\rho U_0 b_0}{\mu}, \frac{y_t}{b_0} \right) \tag{2}$$

For relatively large values of the Reynolds' number pertinent to this study, viscous effects can be neglected (see Rajaratnam 1976; Hager and Bremen 1989), resulting in the simplification of Eq. (2) to

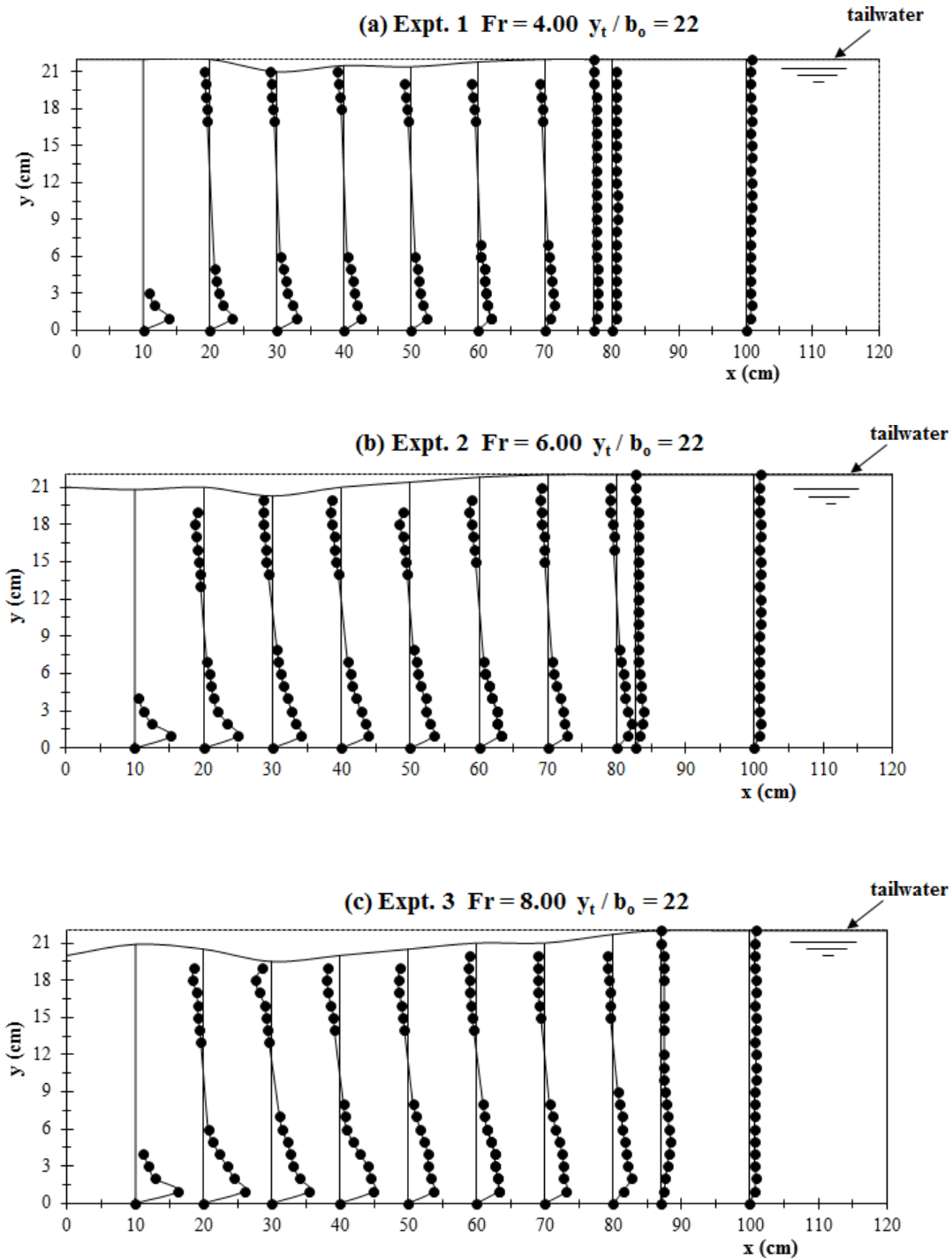
$$\emptyset = f_3 \left(Fr, \frac{y_t}{b_0} \right) \tag{3}$$

Eq. 3 indicates that the primary variables affecting the different characteristics of wall jets are the Froude number and the tailwater depth ratio. This study tested a single tailwater depth ratio and compared it with classical wall jets.

Experimental Results and Analysis:

Fig. 3 (a, b, c, and d) illustrate the results of experiments (1, 2, 3, and 4), respectively. They show the water surface profiles where y is the water depth at any horizontal flow direction distance, x . Also, they represent the results of measurements for the streamwise velocity profiles for a wall jet with a finite tailwater depth. The velocity profiles are drawn at some selected sections with horizontal distances x apart. As mentioned before, the four figures representing the four experiments have the same gate opening ($b_0 = 1$ cm) and tailwater depth ($y_t = 22$ cm). That is the ratio y_t/b_0 is kept constant at 22. However, the Froude number Fr varied with the values of (4, 6, 8, and 10) for experiments (1, 2, 3, and 4), respectively. Water surface profiles were measured from the gate section where $x = 0$ to a section where the flow depth $y = y_t$. For any of the four figures, it is clear that water depth increases gradually with the horizontal distance in the flow developing zone until it reaches y_t approximately at the end of the eddy length, L_e . Comparing the four figures, it is shown that the flow depth at the jet section ($x = 0$) is 22, 21, 20, and 19.5 cm for the jet Froude number equals 4, 6, 8, and 10, respectively. That is the water depth at the jet increases with the decrease of Fr . The peak reverse velocity at any station was observed to occur at or near the water surface. The maximum reverse velocity for any experiment was determined to occur at a distance $L_e / 2$ from the gate as shown in Fig. 4, where L_e is the eddy length. The length of the eddy was also determined by dye injection as shown in Fig. 5. Fig. 6 illustrates the experimental results as a dimensionless eddy length (L_e/b_0) with Froude numbers (Fr). On the other hand, the eddy length increases with the increase of Fr due to the increase of the flow energy. L_e/b_0 can be expressed with the equation.

$$y = 7.99x + 64.72 \quad (r^2 = 0.774) \tag{4}$$



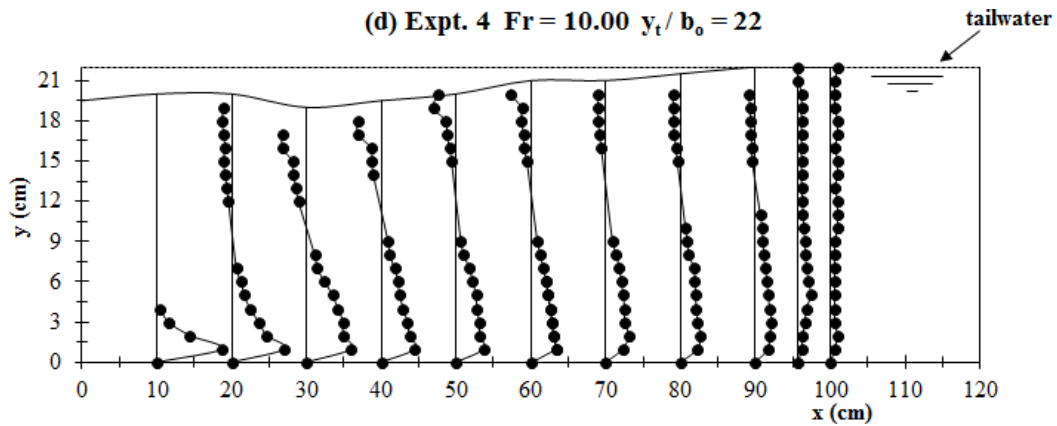


Fig. 3. Typical velocity fields of wall jets in limited tailwater ($y_t/b_o = 22$) for experiments (a) $Fr = 4$; (b) $Fr = 6$; (c) $Fr = 8$; and (d) $Fr = 10$

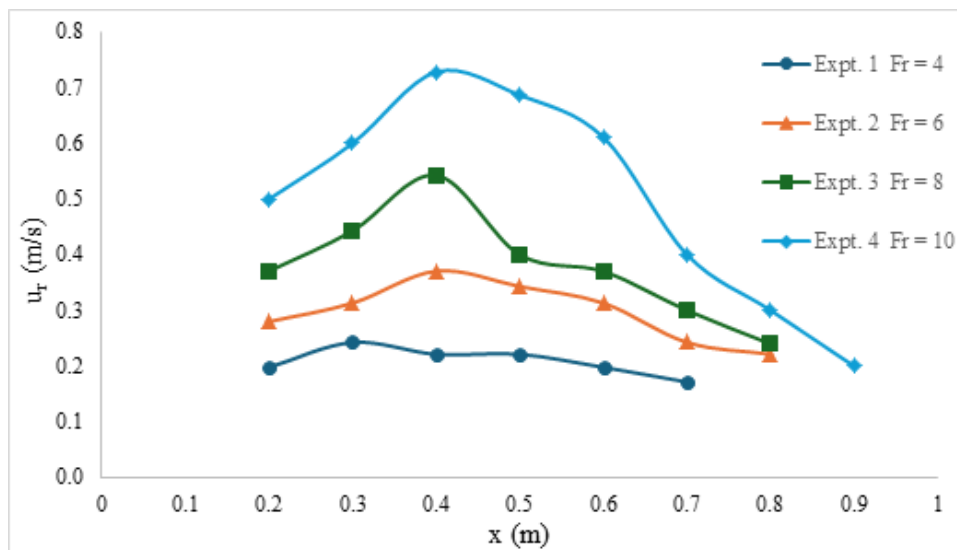


Fig. 4. Variation of maximum reverse velocity with distance



Fig. 5. Expt. 3 with ($Fr = 8$)

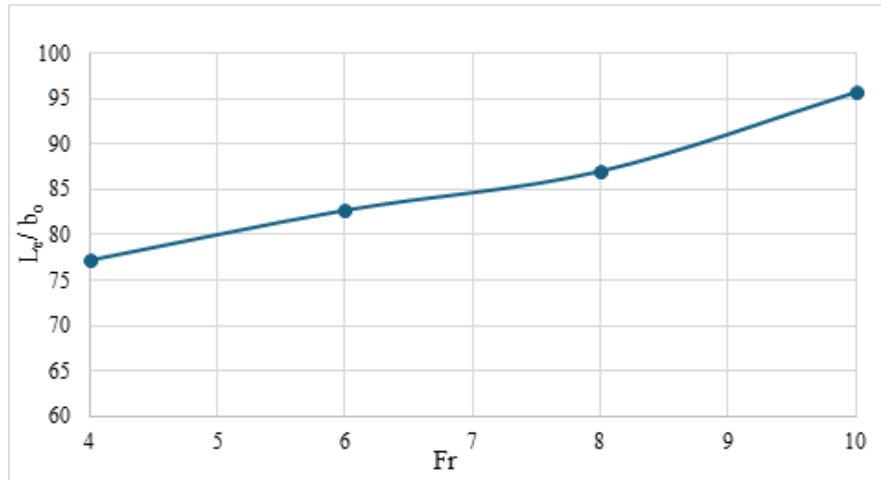


Fig. 6. Illustrates the experimental results as (L_e/b_0) versus (Fr).

The examination of the velocity field reveals that velocity measurements in the forward flow distinctly illustrate the configuration of the wall jet. The maximum velocity, u_m , at any station was chosen as the velocity scale to evaluate the similarity of the velocity profiles, and the length scale, b , is defined as a specified vertical distance y , where $u=0.5u_m$ and $\partial u/\partial y$ is negative. (Fig. 7.a, and 8.a) show velocity profiles for experiments (2, and 3), respectively. It illustrate the relationship between the velocity u for different stations x . (Fig. 7.b, and 8.b) present similarity profiles for the velocity distributions, depicting the variation of the relative streamwise velocity u/u_m with relative vertical distance y/b together with the representation of the velocity profile of the classical wall jet in bold black line. Results showed analogous distributions of the velocity profiles at various stations with the classical wall jet. Velocity profiles for $x/b_0 \leq 12$ were excluded due to their dissimilarity to those presented in (Fig. 7.b, and 8.b). Fig. 9 shows the similarity profiles of the four experimental datasets, excluding the regions near and far from the slot, where the velocity distribution differed from that of wall jets. The similarity profile for the plane turbulent wall jet resembles that of the classical wall jet. However, it's clear that in some areas, the measurements showed more decay compared to the classical wall jets. The discrepancy between the similarity profile for the stream data and the classical wall jet profile is likely due to the shallow tailwater depth. Upon discovering that the velocity profiles in the forward flow exhibit similarity, it is essential to examine the variation of the velocity scale u_m and the length scale b in relation to the distance x .

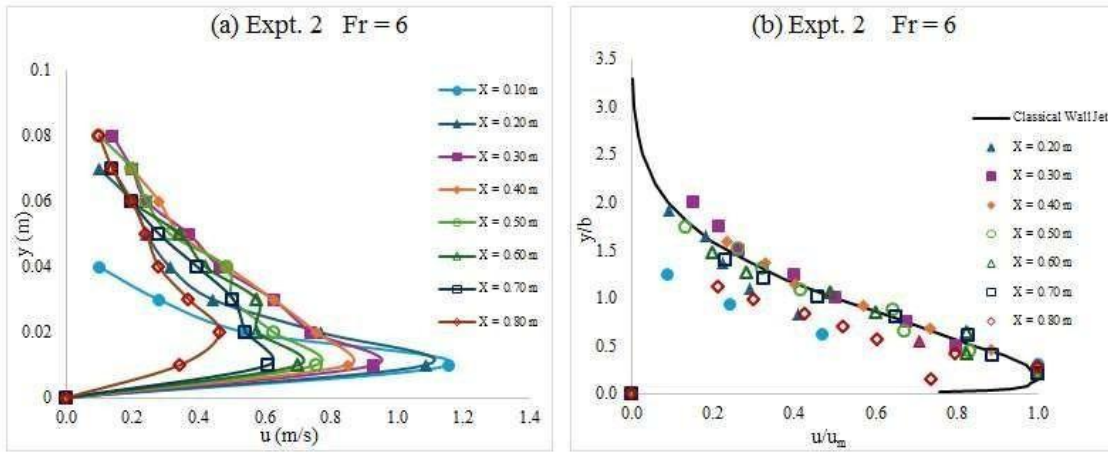


Fig. 7. (a) Velocity distribution for expt. (2 at Fr = 6); (b) Similarity profile for expt. (2 at Fr = 6)

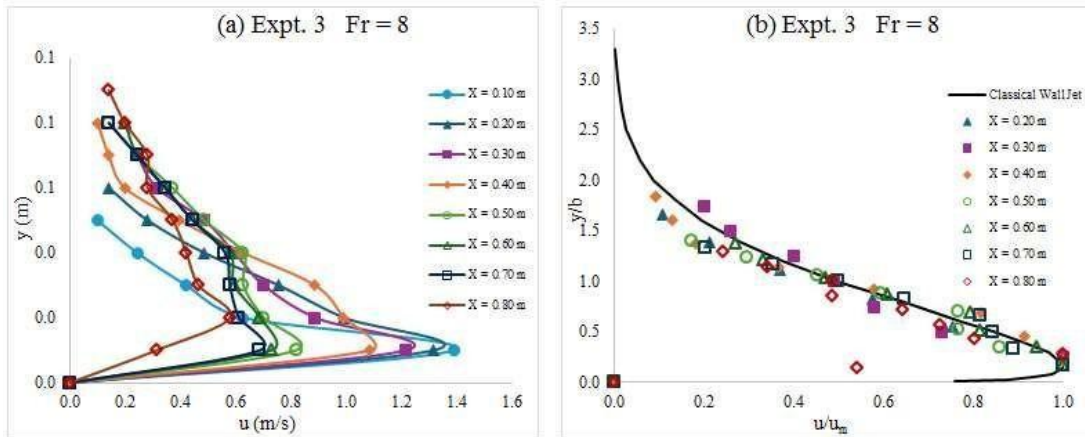


Fig. 8. (a) Velocity distribution for expt. (3 at Fr = 8); (b) Similarity profile for expt. (3 at Fr = 8)

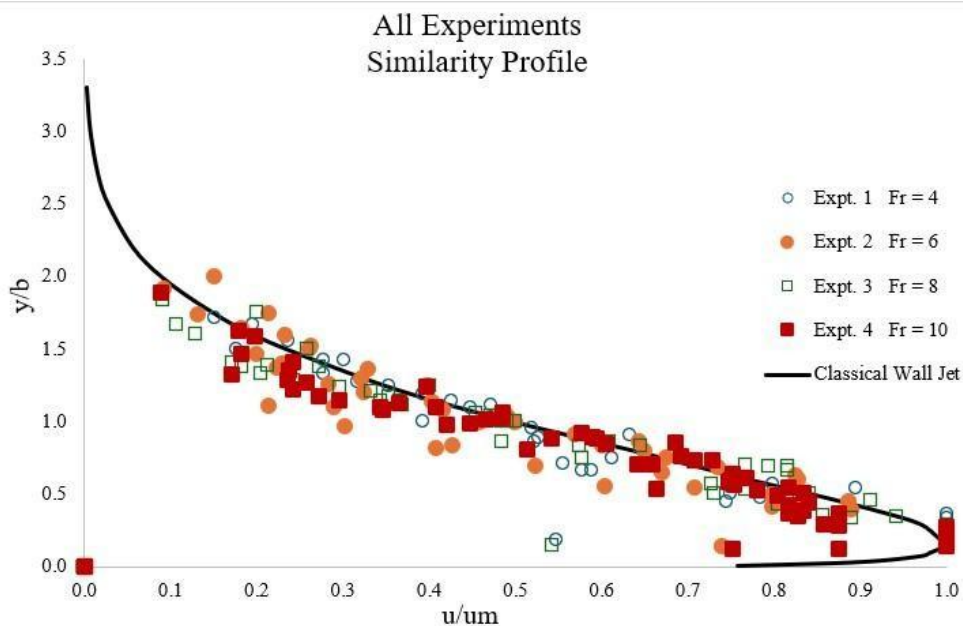


Fig. 9. Similarity profile for all experiments



Fig. 10 (a) depicts the decay of maximum velocity with a longitudinal distance from the slot. The maximum velocity at the slot ranged from 0.71 to 1.57 m/s, and u_m was measured for x up to approximately 0.9 m. Fig. 10 (b) shows the decay of the maximum velocity u_m at any station x normalized by the jet velocity at the slot, U_o , with the relative distance from the gate x/b_o . The plot of maximum velocity decay for classical wall jets is also included. For shallow tailwater depth ratios, the maximum velocity decays more rapidly with distance than for classical wall jets, where the maximum velocity decays gradually for classical wall jets. It was found that with increasing Froude number, the maximum velocity decay increases except for experiment 2 with $Fr = 6$.

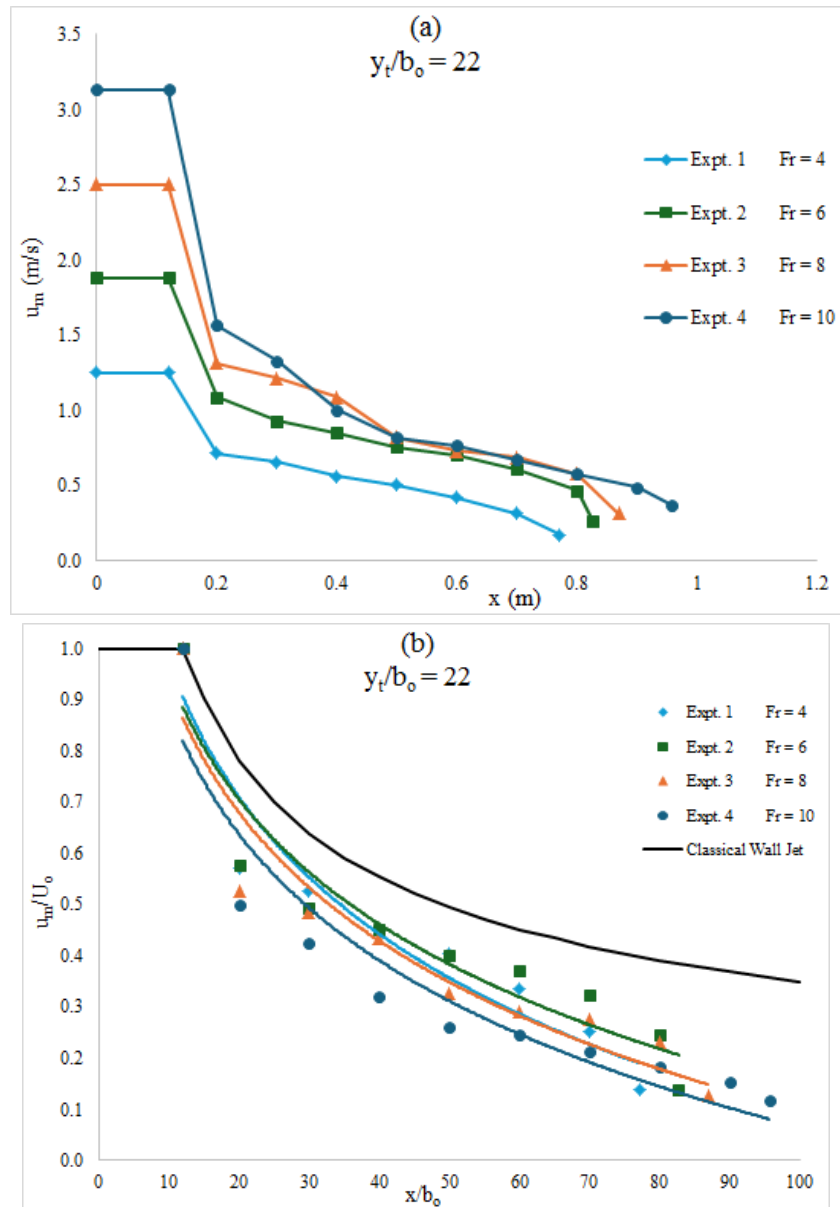


Fig. 10. Variation of the maximum jet velocity with distance (a) u_m against x ; (b) u_m/U_o against x/b_o



Fig.11 shows the growth of the jet's length scale, or half-width b , with distance. This figure also confirms the distinct behavior of the shallow and classical wall jets. Comparing the experimental results representing cases of shallow tailwater wall jets with the classical wall jet (bold black solid line in the figure), it is observed that the jet half-width grows rapidly with distance for shallow tailwater depth ratios ($y_t/b_o = 22$), but slowly for the classical wall jet. Furthermore, the figure displays the results of experiments with different Froude numbers, showing that as the Froude number increases, the jet half-width also increases. In all experiments, at each section where velocity observations were conducted, the forward flow rate Q and the forward momentum flux M per unit width were computed as the aggregate of the fluxes through a thin strip. Fig.12 illustrates the variation of the relative discharge Q/Q_o in the wall jet as a function of the relative distance x/b_o , where Q_o represents the discharge at the slot. An examination of Fig 12. reveals that the behavior of jets with a shallow tailwater depth ratio differs from that of classical wall jets. In the shallow jets ($y_t/b_o = 22$), the relative discharge increases with relative distance at a rate exceeding that of the classical wall jet until a specific section, after which it declines rapidly until it approaches a value of approximately equal 1. The figure also shows that the relative discharge increases with the Froude number until it reaches $Fr = 6$, after which it decreases as the Froude number continues to rise. When the tailwater depth is shallow, the entrainment of recirculating flow with opposing momentum can significantly diminish the wall jet's momentum flux as it moves downstream. Fig.13 shows the variation of the normalized momentum flux of the wall jet with the normalized distance from the nozzle, for both shallow tailwater depth ratios and classical wall jets. The momentum flux experiences a rapid decline in the forward flow up to a specific section, after which it decreases gradually, then declines rapidly once again. The figure also shows that as the Froude number decreases, the momentum flux decreases at a faster rate.

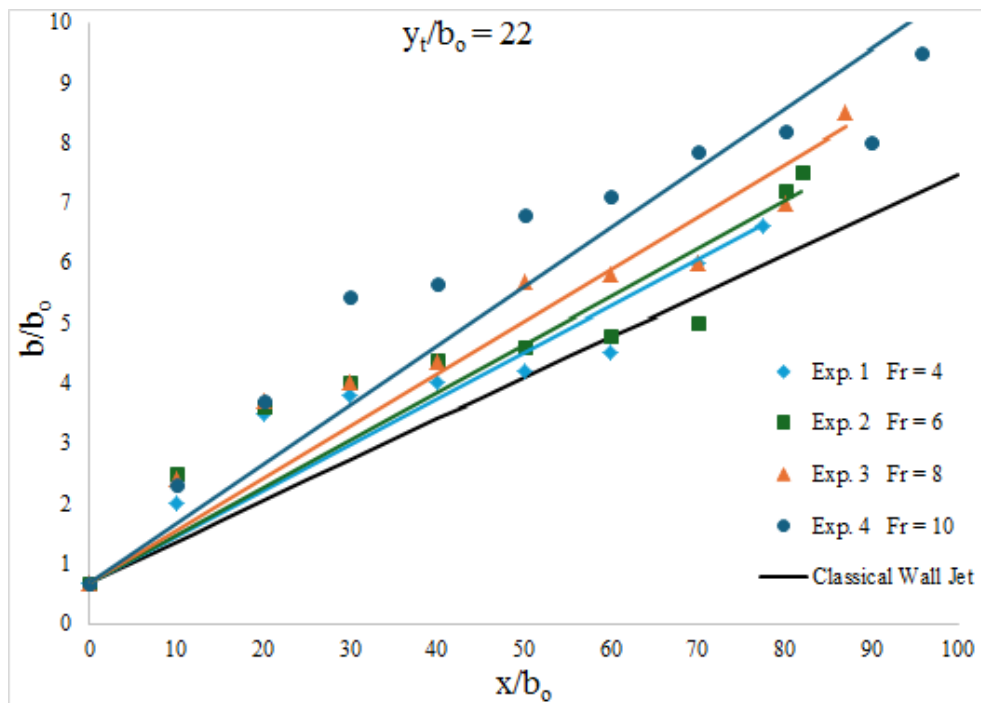


Fig. 11. Variation of jet half-width with distance

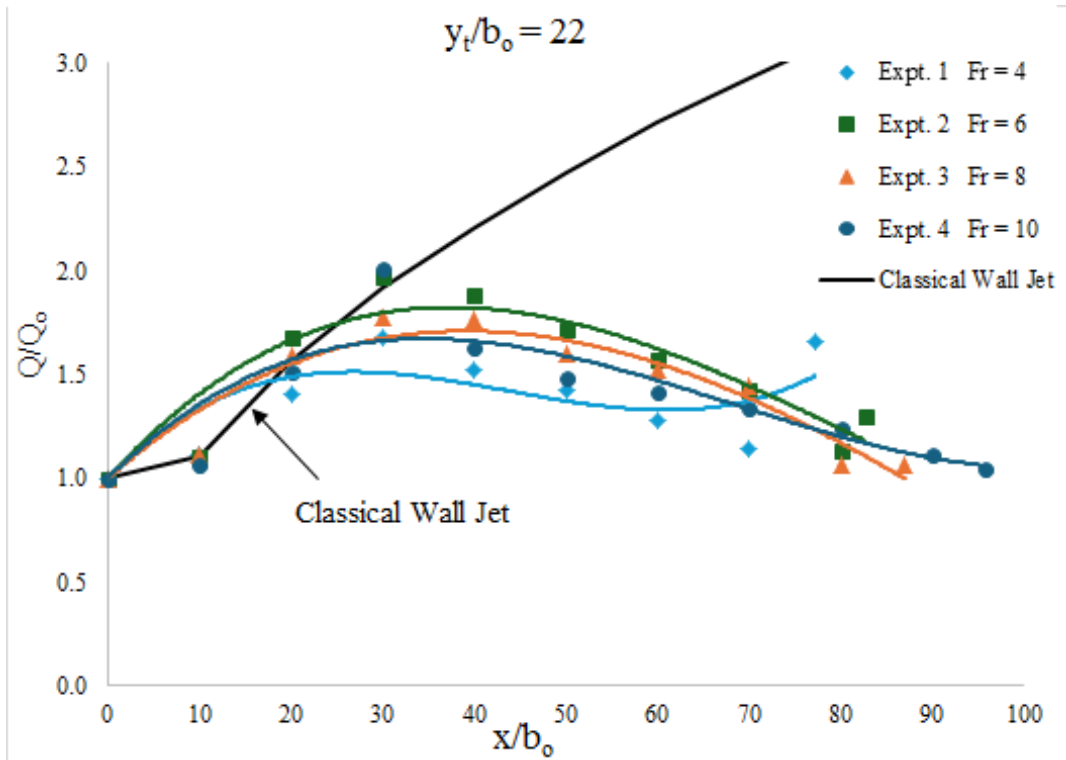


Fig. 12. Variation in wall jet discharge with distance

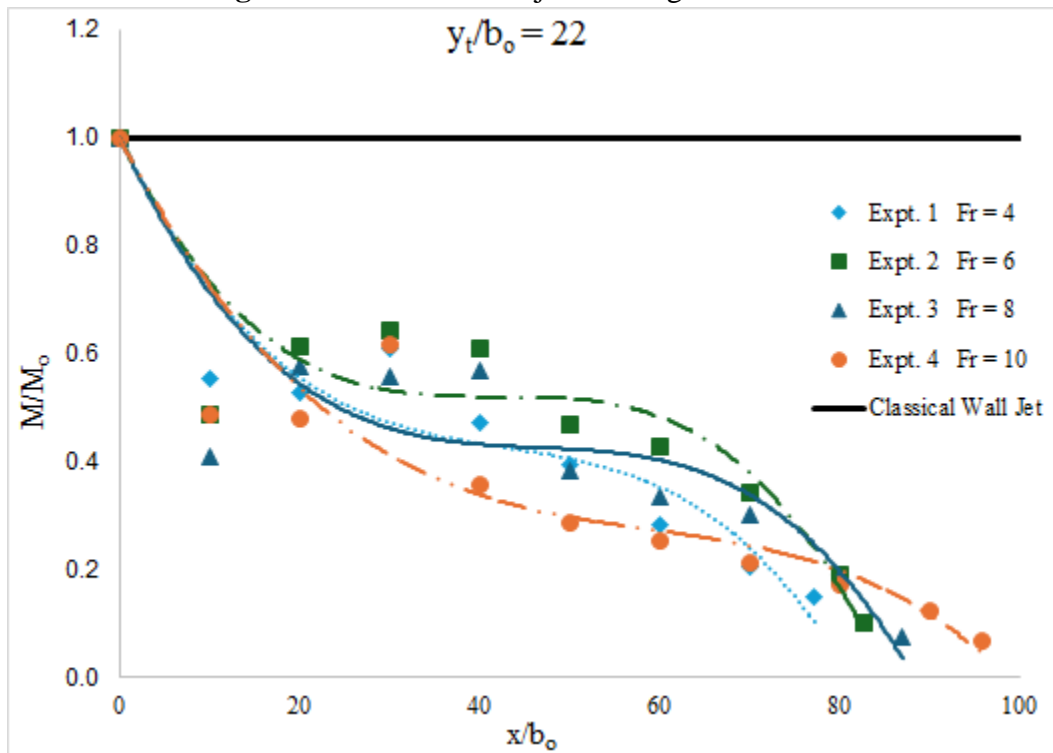


Fig. 13. Variation of wall jet momentum flux with distance.



Conclusion:

In plane turbulent wall jets with limited tailwater depth, a notable distinction exists between the behavior of jets with shallow tailwater depth ratios and that of classical wall jets. The experimental results revealed that for jets with shallow tailwater depth ratios, the maximum velocity decays more quickly than for classical wall jets. and it was observed that when the Froude number increases, the decay of the maximum velocity also increases, except for experiment 2 at $Fr = 6$. In addition, the jet length scale grows at a much faster rate than classical wall jets. And with the increase in the value of the Froude number, the growth of the jet half- width increases. Furthermore, the experimental results demonstrated that for shallower jets, the relative discharge increases with normalized longitudinal distance up to a maximum value before rapidly decreasing to a value of 1 at the end of the eddy length, where the relative discharge of classical wall jets increases much more slowly. Additionally, the relative discharge increases with the Froude number until it reaches $Fr = 6$, after which it declines as the Froude number further increases. The variation of the momentum flux of the forward flow with the normalized longitudinal distance distinguished the shallow and classical wall jets more clearly. The study found that for shallower jets, the momentum flux experiences a rapid decline in the forward flow up to a specific section, after which it decreases gradually, then declines rapidly again. Additionally, the results indicate that the momentum flux decreases at a faster rate as the Froude number diminishes. Overall, the findings of this study highlight the significant effect of the tailwater depth ratio on the behavior of wall jets when compared to classical wall jets.

Reference:

- Forthmann, E. (1936). "Turbulent jet expansion" (No. NACA-TM-789).
- Albertson, M. L., Dai, Y., Jensen, R. A., & Rouse, H. (1950). "Diffusion of submerged jets." *Transactions of the American Society of Civil Engineers*, 115(1), 639-664.
- Miller, D. R., & Comings, E. W. (1957). "Static pressure distribution in the free turbulent jet." *Journal of Fluid Mechanics*, 3(1), 1-16.
- Heskestad, Gunnar. (1965). "Hot-wire measurements in a plane turbulent jet." 721-734.
- Goldschmidt, V., & Eskinazi, S. (1966). "Two-phase turbulent flow in a plane jet." 735-747.
- Kotsovinos, N. E. (1975). "A study of the entrainment and turbulence in a plane turbulent jet." California Institute of Technology, Rep. KH R-32, WM Keck Laboratory of Hydrology and Water Resources, Pasadena, California.
- Kotsovinos, N. E. (1978). "A note on the conservation of the axial momentum of a turbulent jet." *Journal of Fluid Mechanics*, 87(1), 55-63.
- Swean Jr, T. F., Ramberg, S. E., Plesniak, M. W., & Stewart, M. B. (1989). "Turbulent surface jet in channel of limited depth." *Journal of Hydraulic Engineering*, 115(12), 1587-1606.
- Vanvari, M. R., & Chu, V. H. (1974). "Two-dimensional turbulent surface jets of low Richardson number."
- Rajaratnam, N., & Humphries, J. A. (1984). "Turbulent non-buoyant surface jets." *Journal of Hydraulic Research*, 22(2), 103-115.
- Ead, S. A. (1999). "Plane turbulent jets in shallow tailwater and their application to energy dissipation."



- Ead, S. A., & Rajaratnam, N. (2001). "Plane turbulent surface jets in shallow tailwater." *J. Fluids Eng.*, 123(1), 121-127.
- Rajaratnam, N. (1976). "Turbulent jets." Elsevier.
- Javan, M., & Namin, M. (2013). "I D Numerical Simulation of Free Surface in the Case of Plane Turbulent Wall Jets in Shallow Tailwater." In *Civil Engineering Infrastructures Journal* (Vol. 46, Issue 2). www.SID.ir
- Ead, S. A., & Rajaratnam, N. (2002). "Plane turbulent wall jets in shallow tailwater." *Journal of engineering mechanics*, 128(2), 143-155.
- Aziz, T. N., & Khan, A. A. (2011). "Simulation of vertical plane turbulent jet in shallow water." *Advances in Civil Engineering*, 2011(1), 292904.
- Bey, A., Faruque, M. A. A., & Balachandar, R. (2008). "Effects of varying submergence and channel width on local scour by plane turbulent wall jets." *Journal of hydraulic research*, 46(6), 764-776.
- Bhuiyan, F., Habibzadeh, A., Rajaratnam, N., & Zhu, D. Z. (2011). "Reattached turbulent submerged offset jets on rough beds with shallow tailwater." *Journal of Hydraulic Engineering*, 137(12), 1636-1648.
- Shabayek, S. A. (2011). "Plane turbulent wall jets in limited tailwater depth." *International Journal of Engineering & Technology*, 11(6), 192-197.
- Eriksson, J. G., Karlsson, R. I., & Persson, J. (1998). "An experimental study of a two-dimensional plane turbulent wall jet." *Experiments in fluids*, 25(1), 50-60.
- Shinneeb, M., Zouhri, K., & Chikhalsouk, M. (2019, March). "Effect of Shallowness on the Flow Field of a Horizontal Turbulent Water Jet." In *2019 Advances in Science and Engineering Technology International Conferences (ASET)* (pp. 1-6). IEEE.
- Rowland, J. C., Stacey, M. T., & Dietrich, W. E. (2009). "Turbulent characteristics of a shallow wall-bounded plane jet: experimental implications for river mouth hydrodynamics." *Journal of Fluid Mechanics*, 627, 423-449.
- Secchi, F., Gatti, D., & Frohnappfel, B. (2023). "The wall-jet region of a turbulent jet impinging on smooth and rough plates." *Flow, Turbulence and Combustion*, 110(2), 275-299.
- Shivankar, S., Randive, P. R., & Pati, S. (2020). "Effects of undulated wall on the hydrodynamic and thermal transport characteristics of turbulent jet." *International Journal of Thermal Sciences*, 152, 106297.
- Gupta, A., Choudhary, H., Singh, A. K., Prabhakaran, T., & Dixit, S. A. (2020). "Scaling mean velocity in two-dimensional turbulent wall jets." *Journal of Fluid Mechanics*, 891, A11.
- Choudhary, H., Gupta, A., Bhatt, S., Prabhakaran, T., Singh, A. K., Karipot, A., & Dixit, S. A. (2024). "Experimental investigation of the structure of plane turbulent wall jets. Part 1. Spectral analysis." *Journal of Fluid Mechanics*, 988, A42.